University of Pennsylvania

Annual Progress Report: 2011 Nonformula Grant

Reporting Period

July 1, 2013 – June 30, 2014

Nonformula Grant Overview

The University of Pennsylvania received $1,000,000 in nonformula funds for the grant award period June 1, 2012 through August 29, 2014. Accomplishments for the reporting period are described below.

Research Project: Project Title and Purpose

New PET Imaging Agents for Cancer Diagnosis – The purpose of this project is to find new fluorine-18 (F-18) radioactive labeled glutamine derivatives as imaging agents to diagnose cancer. Current diagnosis methods often miss a significant portion of tumor in cancer patients. There is an urgent need to improve cancer diagnosis by introducing new imaging agents for detecting those tumors, which use a different nutrient to thrive. The proposed new F-18 glutamine derivatives will be patent-protected and serve as drug candidates for commercialization. The new drugs will have potential for a wide spread application for cancer diagnosis.

Anticipated Duration of Project

6/1/2012 – 8/29/2014

Project Overview

The objective of this project is to develop specific tumor-targeting imaging agents for cancer diagnosis. The specific aims focus on the preparation and testing of novel fluorine-18 (F-18) labeled glutamine derivatives as candidates for commercial drug development. Currently, positron emission tomography (PET) imaging, which uses the glucose derivative F-18 labeled 2-fluoro-2-deoxy-glucose (FDG), is the method of choice in tumor diagnosis. A growing tumor consumes a higher amount of glucose than normal tissue, so excessive FDG uptake is mapped by FDG-PET imaging. Recently, it was discovered that some rapidly growing tumors do not take up glucose. In order to grow continuously, many tumors use glutamine, an amino acid with a high concentration in blood, as their source nutrient. These tumors therefore cannot be detected by FDG-PET imaging. The inability to detect these tumors has a critical impact in real life: increased cancer mortality. To improve cancer diagnosis, we will design and evaluate novel glutamine derivatives, which mimic glutamine. The new glutamine-based drug candidates will be patentable new chemical entities. They will receive worldwide patent protection and thus will

attract additional private venture funding for commercial development. The Office of Technology Transfer at the University of Pennsylvania will file the US patents and serve as the holder of intellectual properties. A newly established Philadelphia-based company will license the technology for further commercial development. The project will not only discover new drug candidates but also will facilitate the establishment of a new company to develop and market the new drugs. This is an excellent opportunity to create a more effective means of cancer diagnosis; it will also provide economic benefits for the region. It is worth noting that in 2004 the PI cofounded Avid Radiopharmaceuticals, Inc. in the University City Science Center, Philadelphia to develop PET imaging agents for diagnosis of neurodegenerative diseases. Avid Radiopharmaceuticals, Inc. has completed a phase III clinical trial for a new F-18 PET imaging agent, florbetapir f 18, for imaging amyloid plaques in patients at risk of developing Alzheimer's disease. Eli Lilly and Company acquired Avid Radiopharmaceuticals, Inc. in 2010. The PI's previous success in bringing new imaging drugs from the laboratory to the market will serve this project well.

Specific Aims:
Specific Aim 1: Proof of principal for the proposed new drug candidates, [^{18}F]4-fluoro-glutamine derivatives
Specific Aim 2: In vivo stability in rodent tumor models at least one compound

Principal Investigator

Hank F. Kung, PhD
Professor
University of Pennsylvania
3700 Market Street, Room 305
Philadelphia, PA 19104

Other Participating Researchers

Mitchell Schnall, MD, PhD; Karl Ploessl, PhD; Daniel A. Pryma, MD – employed by the University of Pennsylvania

Expected Research Outcomes and Benefits

The proposed project will synthesize and test a series of fluorine-18 labeled glutamine derivatives as imaging agents for detecting tumor growth. We expect that this project will produce two new drug candidates suitable for commercial development. The potential outcome will be to improve cancer diagnosis, thereby providing a widespread benefit to current and future cancer patients. A newly established Philadelphia-based company will license the technology for further commercial development. The expected outcome of this commercialization will be both the manufacture and distribution of novel cancer imaging agents, as well as potential economic benefits to the Philadelphia region in the form of new jobs.

Summary of Research Completed

Specific Aim 1 milestones for reporting period:

We will test at least one drug candidate (from Group A) in rodent model with one drug candidate feasible for moving to the next level.

1a. chemical synthesis of "cold" glutamine derivatives

1b. study the in vitro stability of "cold" glutamine derivatives

1c. testing the radiolabeling and improve radiolabeling yields

1d. study the in vitro stability of "hot" glutamine derivatives

Specific Aim 2 milestones for reporting period:

2a. biodistribution studies in rodent tumor models

2b. in vivo PET imaging studies in rodent tumor models

While the growth and proliferation of most tumors is fueled by glucose, some tumors are more likely to metabolize glutamine. In particular, tumor cells with the upregulated c-Myc gene are generally reprogrammed to utilize glutamine. We have developed new 3-fluoropropyl analogs of glutamine, namely [^{18}F](2*S*,4*R*) and [^{18}F](2*S*,4*S*)4-(3-fluoropropyl)glutamine, **3** and **4**, to be used as probes for studying glutamine metabolism in these tumor cells. Optically pure isomers labeled with ^{18}F and ^{19}F (2*S*,4*S*) and (*2S,4R*)4-(3-fluoropropyl)glutamine were synthesized via different routes and isolated in high radiochemical purity (≥ 95%). Cell uptake studies of both isomers showed that they were taken up efficiently by 9L tumor cells with a steady increase over a timeframe of 120 minutes. At 120 minutes their uptake was approximately two times higher than that of L-[^{3}H]glutamine ([^{3}H]Gln). These *in vitro* cell uptake studies suggested that the new probes are potential tumor imaging agents. Yet, the lower chemical yield of the precursor for **3,** as well as the low radiochemical yield for **3**, limits the availability of [^{18}F](2*S*,4*R*)4-(3-fluoropropyl)glutamine, **3.** We therefore focused on [^{18}F](2*S*,4*S*)4-(3-fluoropropyl)glutamine, **4**. The *in vitro* cell uptake studies suggested that the new probe, [^{18}F](2*S*,4*S*)4-(3-fluoropropyl)glutamine, **4**, is most sensitive to the LAT transport system, followed by System N and ASC transporters. A dual-isotope experiment using L-[^{3}H]glutamine and the new probe showed that the uptake of [^{3}H]Gln into 9L cells was highly associated with macromolecules (>90%) while the [^{18}F](2*S*,4*S*)4-(3-fluoropropyl)glutamine, **4**, was not (< 10%). This suggests a different mechanism of retention. *In vivo* PET imaging studies demonstrated tumor-specific uptake in rats bearing 9L xenographs with an excellent tumor to muscle ratio (maximum of ~ 8 at 40 minutes). [^{18}F](2*S*,4*S*)4-(3-fluoropropyl)glutamine, **4**, may be useful for testing tumors that may metabolize glutamine related amino acids.

One of the drawbacks of [^{18}F](2*S*,4*R*)4-FGln, **2**, (and its related optical isomers) is the radiolabeling reaction, which is relatively difficult and prone to formation of stereo-isomers due a secondary fluorination reaction. To avoid this complication, we have designed and tested [^{18}F](2*S*,4*R*)4-(3-fluoropropyl)glutamine, **3** ([^{18}F](2*S*,4*R*)4-FPGln) and [^{18}F](2*S*,4*S*)4-(3-fluoropropyl)glutamine, **4** ([^{18}F](2*S*,4*S*)4-FPGln), as alternative probes for imaging glutamine metabolism (Figure 1). The 4-(3-fluoropropyl)glutamines contain an extended propyl group. This will make it easier for the SN_2 fluorine substitution with a good leaving group (-OTs) used in the labeling reaction. To preserve the amide functional group at the C5 position, we have

synthesized two types of precursors suitable for radiolabeling (fluoro-for-tosylate substitution reaction).

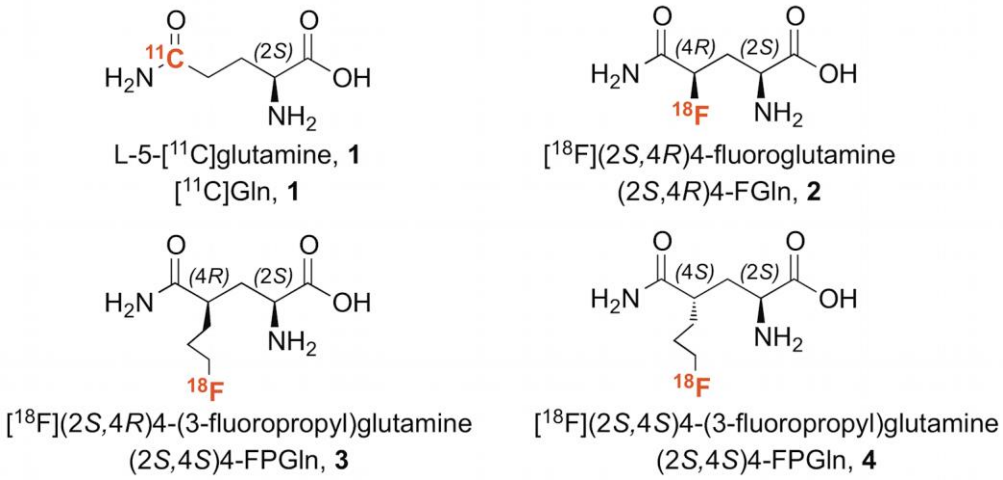

Figure 1. Chemical structures of L-5-[11C]glutamine, 1, (11C]Gln), [18F](2S,4R)4-fluoroglutamine, 2 ([18F](2S,4R)4-FGln), [18F](2S,4R)4-(3-fluoropropyl)glutamines, 3, ([18F](2S,4R)4-FPGln) and [18F](2S,4S)4-(3-fluoropropyl)glutamines, 4, ([18F](2S,4S)4-FPGln).

In order to produce [^{18}F](2*S*,4*R*)4-(3-fluoropropyl)glutamine, **3**, ([^{18}F](2*S*,4*R*)4-FPGln) and [^{18}F](2*S*,4*S*)4-(3-fluoropropyl)glutamine, **4**, ([^{18}F](2*S*,4*S*)4-FPGln) we employed two different schemes (Scheme 1 and 2) for preparation of non-radioactive "cold" compounds (**3** and **4**) and the cyanide and –OTs precursors for radiolabeling. One approach was to prepare the corresponding protected 4-cyanide derivatives, which led to the formation of the desired final products. Commercially purchased Boc-Asp(OBzl)-OH, **5**, was treated with *tert*-butyl 2,2,2-trichloroacetimidate/$BF_3 \cdot Et_2O$ at room temperature to give the t-BuO- ester, **6**; the BnO- ester group was converted to the acid, **7**, by Pd/C catalyzed hydrogenation. The aspartic acid, **7**, was carefully reduced with $NaBH_4$ in THF/water at -15 ^oC to 0 ^oC to the corresponding alcohol, **8**. The alcohol group was successfully converted to the cyanide, **10**, through the O-Ts intermediate, **9**. The cyanide derivative, **10**, was treated with LiHMDS and allyl bromide at -78 ^oC to give (2*S*,4*S*)-*tert*-butyl 2-(*tert*-butoxycarbonylamino)-4-cyanohept-6-enoate (**11a**) and (2*S*,4*R*)-*tert*-butyl 2-(*tert*-butoxycarbonylamino)-4-cyanohept-6-enoate (**11b**) (**11a** to **11b** ratio of 2:1 in 28% and 15% isolated yields). A similar reaction was reported previously for preparation of allyl derivatives of aspartate using the dianionic allylation reactions of amino acid derivatives. The allyl derivatives, **11a** and **11b**, were separated and purified by flash chromatography. They were converted to the corresponding alcohols, **12a** and **12b**, and following the treatment with tosyl chloride to the O-tosylated, **13a** and **13b** in good yields. The O-tosylated, **13a** and **13b** were treated with TASF, $Et_3N(HF)_3$, DCM, DMF, 50 ^oC, overnight to give the desired **14a** and **14b,** in good yields. Optimization of the fluorination reaction condition using TASF and $Et_3N(HF)_3$, as the reagents was reported previously for the preparation of 4-fluoroglutamine. De-protection using hydrochloric acid at room temperature produced the final end products, [^{18}F](2*S*,4*R*)4-(3-

fluoropropyl)glutamine, **3** and [^{18}F](2*S*,4*S*)4-(3-fluoropropyl)glutamine, **4**. The O-tosylated, **13a** and **13b** were also successfully used for the radiolabeling reaction

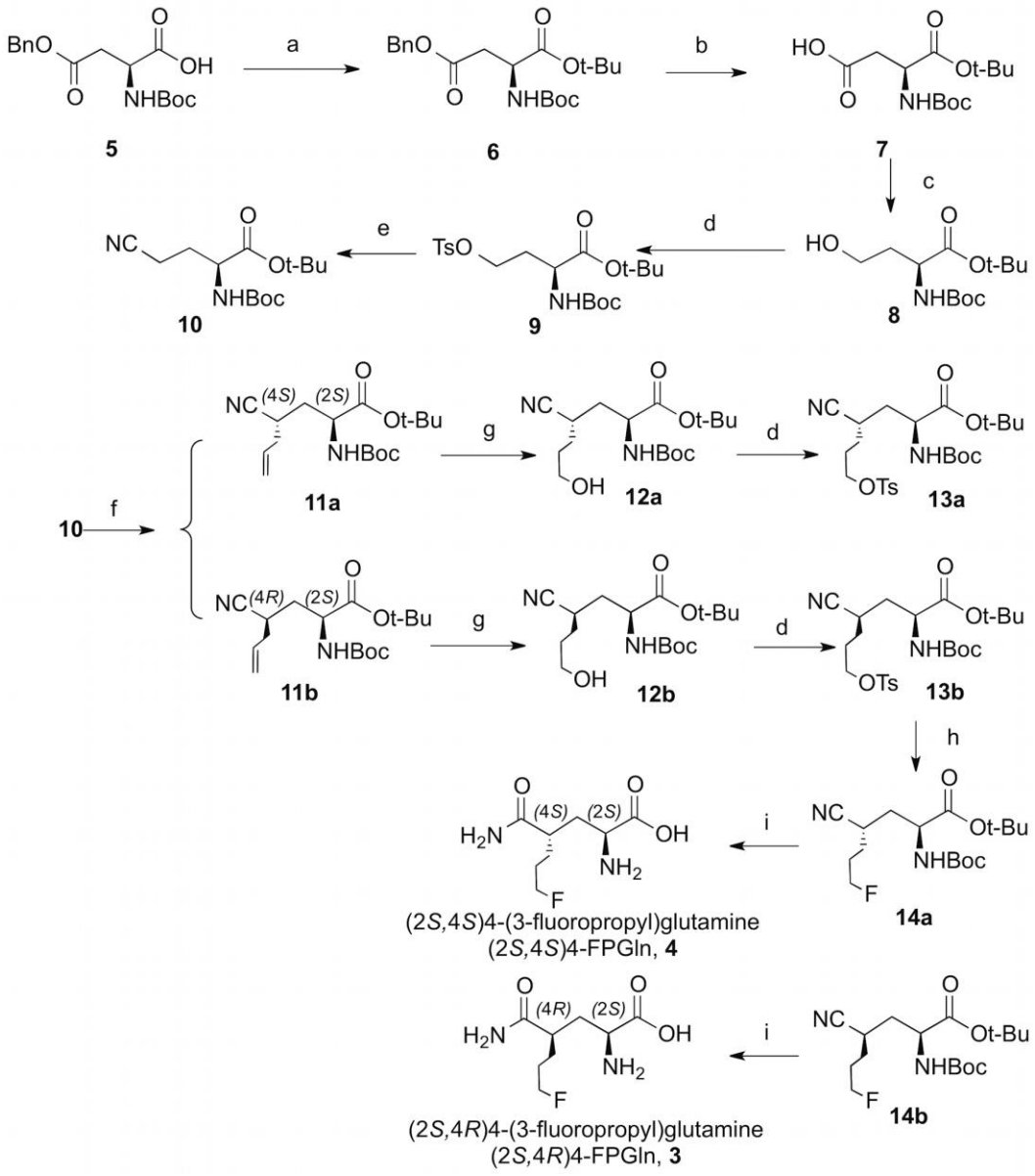

Scheme 1. Reagents and reaction conditions: a) tert-butyl 2,2,2-trichloroacetimidate (TBTA), BF3•Et2O, DCM, cyclohexane, rt, overnight; b) Pd/C, H2, MeOH, rt, overnight; c) ECF, NaBH4, THF, H2O, -15 - 0 oC, 4 h; d) TsCl, Et3N, DMAP, DCM, rt, overnight; e) NaI, KCN, DMF, rt, overnight; f) LiHMDS, Allyl bromide, THF, -78 oC, 4 h; g) 9-BBN, H2O2, NaOH, 0 oC - rt, 48 h; h) TASF, Et3N(HF)3, DCM, DMF, 50 oC, overnight; i) HCl, rt, 6 h.

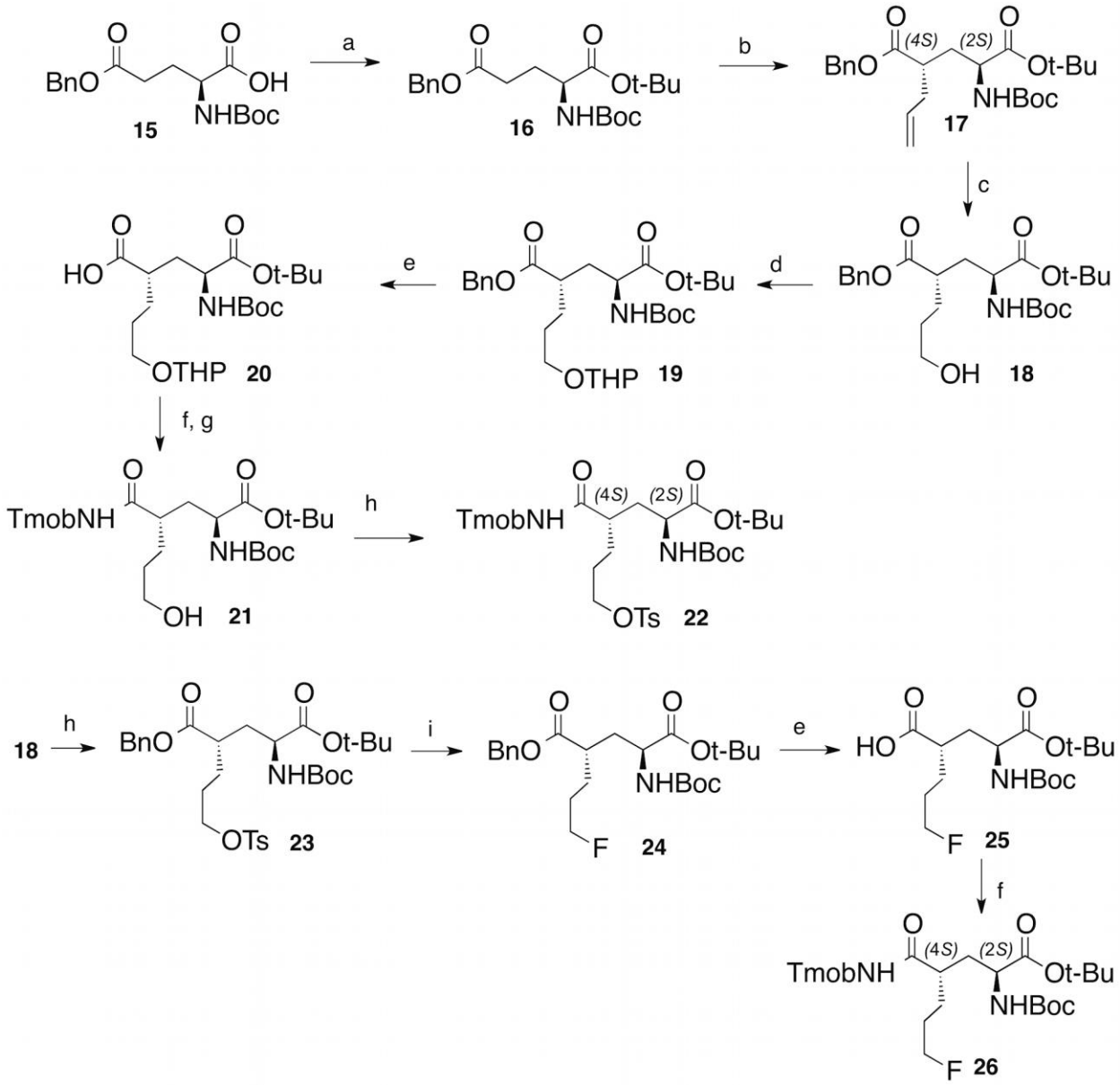

Scheme 2. Reagents and conditions: a) tert-butyl 2,2,2-trichloroacetimidate (TBTA), BF3•Et2O, DCM, cyclohexane, rt, overnight; b) LiHMDS, Allyl bromide, THF, -78 oC, 4 h; c) 9-BBN, H2O2, NaOH, 0 oC - rt, 48 h; d) DHP, PPTS, DCM, rt, 3 h; e) Pd/C, H2, EtOH, rt, 6 h; f) TmobNH2•HCl, EDCI•HCl, HOBt, Et3N, DCM, DMF, rt, 24 h; g) PPTS, EtOH, 50 oC, 4 h; h) TsCl, Et3N, DMAP, DCM, rt, overnight; i) TASF, Et3N(HF)3, DCM, DMF, 50 oC, overnight.

The second method introduced N-Tmob protected precursors (as a protecting group to preserve the amide) for radiolabeling and deprotection. Previously, we have tested for the preparation of N-Tmob protected precursors for making isomers of 4-fluoroglutamine (4-FGln) 9. We successfully developed 18F labeling using this precursor under different labeling conditions. We

wanted to extend the same method to the synthesis and labeling of [18F](2S,4S)4-(3-fluoropropyl)-glutamine, 4. To achieve this, we started with commercially available, Boc-Glu(OBzl)-OH, 15. After treating with tert-butyl 2,2,2-trichloroacetimidate/BF3•Et2O at room temperature, it gave the t-Bu ester, 16. Using the same dianionic allylation reactions of amino acid derivatives 14, the reaction preferentially produced the protected (2S,4S)4-allyl-glutamate (in 58% yield). It is interesting to note that the reaction led to the (2S,4S) isomer only. The allyl group was converted to alcohol, 18, by 9-BBN/H2O2/NaOH in 0 oC. The alcohol was protected by THP, and the O-Benzyl ester was hydrolyzed and the acid, 20, was transformed to Tmob-protected amide, 21. The alcohol, 21, was treated with tosyl chloride to the O-tosylated, 22, which is a suitable precursor for a radioactive 18F labeling reaction. In order to provide an authentic sample, a cold standard, for the first step of the radioactive 18F labeling reaction, we also prepared compound, 26.

To further confirm the chemical structure, a slow evaporating recrystallization method provided excellent crystals of "cold" (2S,4S)4-FPGln, 4 and the X-ray crystallographic analysis data added support to the structure assignment (Figure 2). The optically pure (2S,4S)4-FPGln, 4, has never been prepared and presented before. In the X-ray crystallographic structures of (2S,4R)4F-Gln, 2 and (2S,4S)4-FPGln, 4, the amino acid groups on the right side of the molecules were comparable; while the amide group on the left appeared to be varied and different from each other. The results reported in Figure 2 firmly establish the configuration, which may facilitate future use of other 4-fluoroglutamine isomers for biological and medical applications.

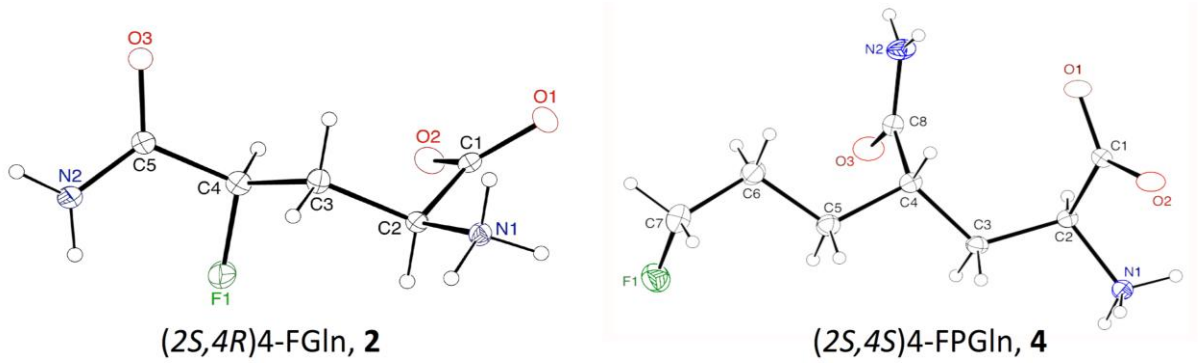

Figure 2. Comparison of x-ray crystallography structures for (2S,4R)4-fluoro-glutamine, (2S,4R)4-FGln, 2 9 and (2S,4S)4-(3-fluoropropyl)glutamine, (2S,4S)4-FPGln, 4. ORTEP drawing of the title compounds were shown with 30% probability thermal ellipsoids. (Crystal structure, (2S,4S)4-FPGln, 4, was submitted to the Cambridge Crystallographic Data Centre (CCDC 991692).

Radiolabeling of the desired [^{18}F](2*S*,4*R*)4-FPGln, **3** and [^{18}F](2*S*,4*S*)4-FPGln, **4**, was achieved by methods in Scheme 3. The preparation can be accomplished by using the O-tosylated cyanide derivatives, **13a** or **13b**, or the O-tosylated TmobNH- protected precursor, **22**. The substitution of O-Ts with [^{18}F]fluoride using O-tosylated cyanide derivatives, **13a** or **13b**, was performed with 18-crown-6/$KHCO_3$ in DMSO at 110 ºC for 10 min, followed by a solid-phase extraction

(Oasis® HLB 3cc cartridge). The intermediate was eluted from this cartridge and treated with H_2SO_4/TFA at 120 ºC for 10 min. The crude labeled products were cooled to room temperature and neutralized with a sat. Na_2CO_3 solution. The mixture was passed through an Oasis® HLB 3cc cartridge topped with Ag11-A8 resin. The cartridge was eluted with phosphate buffered saline (pH 7.0) to give the desired radioactive [^{18}F](2*S*,4*R*)4-FPGln, **3** and [^{18}F](2*S*,4*S*)4-FPGln, **4**, respectively (Scheme 3). The purity was measured with reversed-phase HPLC (radiochemical purity) and chiral HPLC (optical purity). The decay corrected radiochemical yield was 6.2 ± 3.9%, radiochemical purity 91.5 ± 1.5%, optical purity > 99 %, n = 2 (for **3**) and 25.2 ± 2.3%, RCP 92.8± 2.6%, optical purity > 99 %, n = 5 (for **4**). It is important to note that radiolabeling of these two seemingly close analogs showed very different yields. We noted the disparity in radiolabeling yields, but we do not have a simple explanation for this phenomenon. Additional studies may be needed to investigate the optical preferences in the substitution of O-Ts with [^{18}F]fluoride. To improve the radiolabeling reaction for the more promising [^{18}F](2*S*,4*S*)4-FPGln, **4**, we made the effort to use a different O-tosylated TmobNH- protected precursor, **22**. A similar 4-O-tosylated TmobNH-protected precursor was successfully employed for substitution of O-Ts with [^{18}F]fluoride using similar reaction conditions to give the desired [^{18}F](2*S*,4*R*)4-FGln, **2**, in good radiochemical yields (30 - 40%). However, much to our surprise the radiochemical yield for precursor, **22**, gave a lower labeling yield. The decay corrected radiochemical yield was 2.7 ± 0.9%, n = 3.

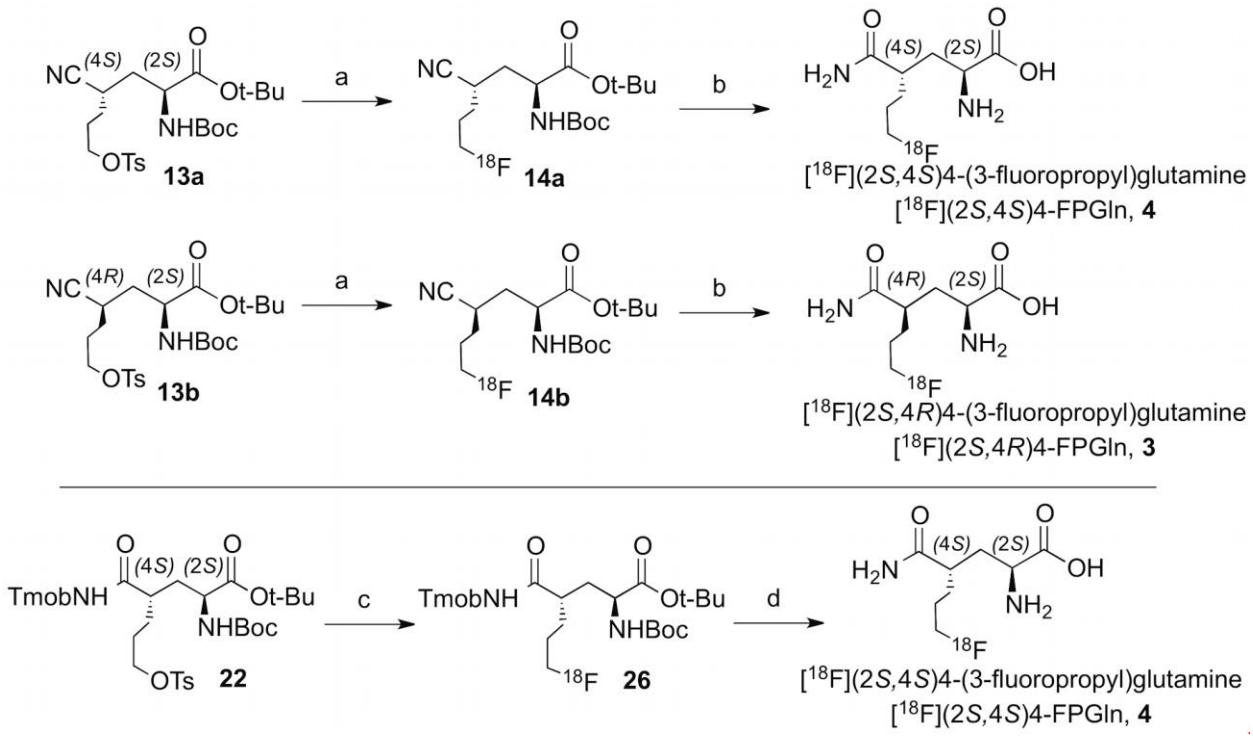

Scheme 3. Procedures for radiolabeling of [18F](2S,4R)4-FPGln, 3 and [18F](2S,4S)4-FPGln, 4. Reagent and conditions: a) 18-crown-6/KHCO3/18F-/DMSO, 110 ºC, 10 min; b) 400 µL TFA/100 µL H2SO4 concentrated/120 ºC, 10 min; c) 18-crown-6/KHCO3/18F-/ACN, 80 ºC, 20 min; d) 500 µL TFA/40 ºC, 8 min.

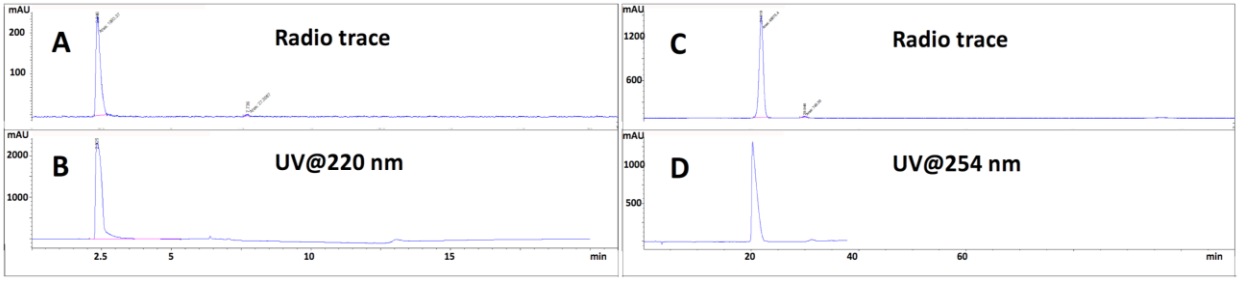

Figure 3. HPLC profiles of [18F](2S,4S)4-FPGln, 4. Profiles A and B were obtained using a gradient system: Gemini 3u C18 150 × 4.6 mm; Gradient, 1 mL/min; Solvent A: ACN, solvent B: 0.1% aqueous formic acid: 0 – 3 min 95% B, 3 – 11 min 95% - 5% B, 11 - 19 min 5% - 95% B, 19 - 21 min 95% B. Profiles C and D were obtained using a chiral column and isocratic system: Chirex 3126 (D)-penicillamine 250 × 4.6 mm, 2 mM CuSO4 solution, 1 mL/min, column temperature at 30 ºC. The radioactive peak displayed the same retention time as that of the "cold" standard under the same HPLC conditions.

In order to test the specificity of this radiotracer, *in vitro* cell uptake and inhibition studies were performed in 9L cells. Both [^{18}F](2*S*,4*R*)4-FPGln, **3**, and [^{18}F](2*S*,4*S*)4-FPGln, **4**, displayed excellent uptake in the 9L tumor cells *in vitro*. At all time-points studied (5 to 120 min) both tracers displayed very similar values (Figure 4). It appeared that the stereo-isomers 4*S* and 4*R* have comparable tumor cell uptakes. Because of this observation, we only used the [^{18}F](2*S*,4*S*)4-FPGln, **4**, tracer in further investigations on inhibition of cell uptakes and for the *in vivo* biological studies. The tracer, [^{18}F](2*S*,4*S*)4-FPGln, **4**, was incubated at 37 °C for 30 minutes with different amino acid transport inhibitors. The results in Figure 5 suggested that system A inhibitor, MeAIB (*N*-methyl-α-aminoisobutyric acid), had no inhibitory effect on the uptake, indicating that the system A amino acid transport was not involved in the uptake of this new tracer. System L inhibitor, BCH (2-amino-bicylo[2.2.1] heptane-2-carboxylic acid), System ASC inhibitor L-serine (L-Ser) and System ASC (SLC1A5), N inhibitor, L-glutamine (L-Gln), exhibited similar concentration dependent reduction of cell uptake, thus indicating potential involvement of system L, ASC and N in the uptake (Figure 5).

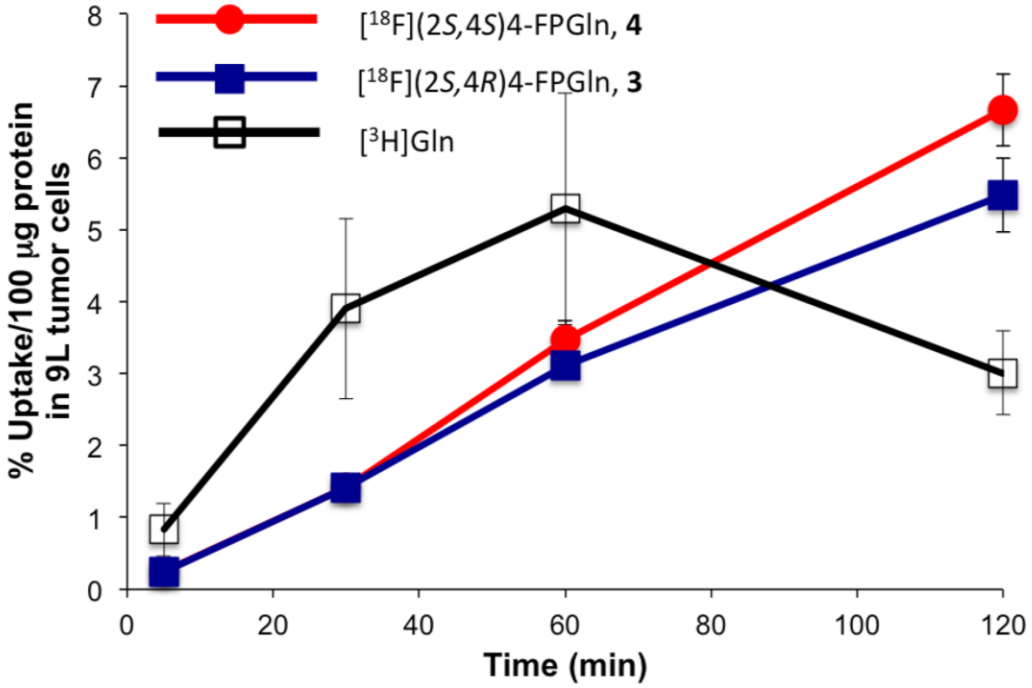

Figure 4. *In vitro* cell uptakes of [^{18}F](2*S*,4*R*)4-FPGln, **3**, and [^{18}F](2*S*,4*S*)4-FPGln, **4**. [^{3}H]Gln was used as a standard. All radiotracers were evaluated in the 9L tumor cell line.

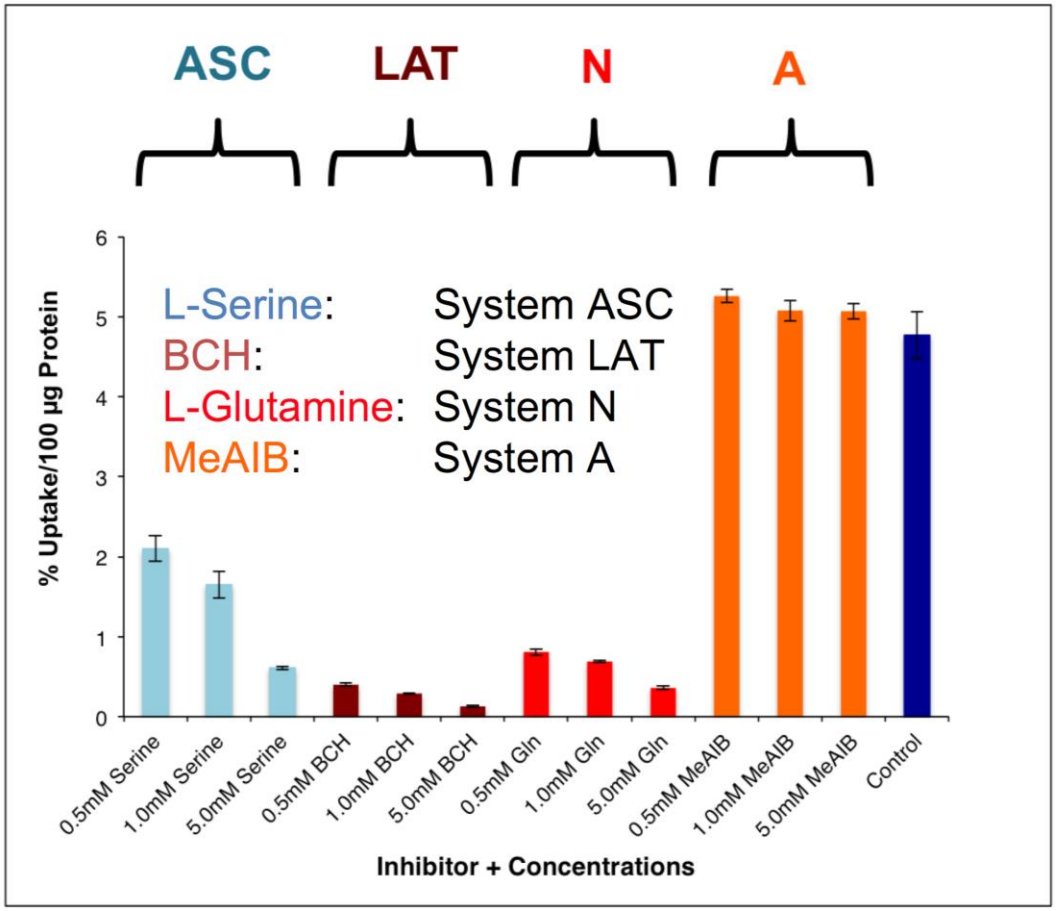

Figure 5. *In vitro* cell uptake inhibition studies of [^{18}F](2*S*,4*S*)4-FPGln, **4,** conducted in 9L cells using inhibitors: System LAT inhibitor, BCH (2-amino-bicylo[2.2.1] heptane-2-carboxylic acid); System ASC inhibitor, L-serine (L-ser), System A inhibitor, N-methyl-α-aminoisobutyric acid (MeAIB); and system N inhibitor, L-glutamine (L-Gln).

*Protein incorporation of [^{18}F](2S,4S)4-FPGln, **4**, into 9L tumor cells*

One of the important issues to consider when developing tracers to image glutamine metabolism in tumors is the protein incorporation of the tracer once inside the cells. After incubation of [^{18}F](2*S*,4*S*)4-FPGln, **4** and [^{3}H]Gln with 9L tumor cells, the cell lysates were treated with TCA and the radioactivity in the precipitates and supernatant were counted. Results showed that the majority of [^{3}H]Gln activity was associated with the TCA precipitates suggesting that most of the [^{3}H]Gln (> 90%) was incorporated into macromolecules, while the glutamine analog, [^{18}F](2*S*,4*S*)4-FPGln, **4**, remained predominantly in the supernatant (no incorporation).

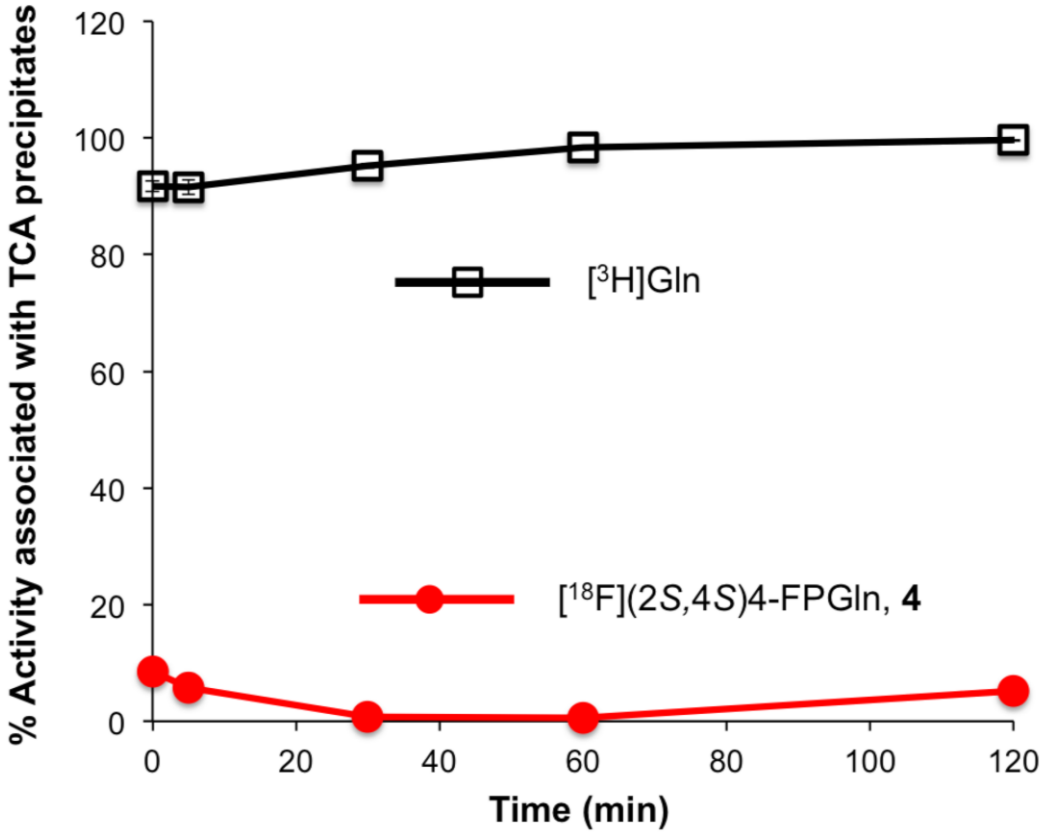

Figure 6. The incorporation of [^{18}F](2*S*,4*S*)4-FPGln, **4**, and [^{3}H]Gln into protein in 9L tumor cells was investigated. The comparison of cellular uptake of [^{18}F](2*S*,4*S*)4-FPGln, **4**, and [^{3}H]Gln was performed using dual-isotope experiments at 0, 5, 30, 60 and 120 min incubation time periods. Cell lysates were treated with TCA and the radioactivity (both ^{18}F and ^{3}H) associated with the TCA precipitates was counted.

Based on the protein incorporation data above (Figure 6), [^{18}F](2*S*,4*S*)4-FPGln, **4**, behaved very differently from that of [^{3}H]Gln. It is reasonable to conclude that the new probe, [^{18}F](2*S*,4*S*)4-FPGln, **4**, is not associated with intra-cellular macromolecules and thus, it is less likely to measure the intracellular metabolism associated with glutamine metabolism.

Biodistribution studies of [^{18}F](2*S*,4*S*)4-FPGln, **4**, were conducted in F344 rats (125 - 149 g, n = 4) bearing 9L tumors on their thigh. This is a well-established animal model that resembles typical human glioblastomas in clinical settings. Rats were sacrificed at 30 and 60 minutes post-injection by cardiac excision while under isoflurane anesthesia. [^{18}F](2*S*,4*S*)4-FPGln, **4**, showed respectable uptake within the 9L tumors, displaying 0.83% dose/g uptake at 30 minutes post injection. Tumor uptake and retention slowly washed out of the 9L tumor to 0.60% dose/g. At 30 minutes, tumor-to-background (tumor-to-muscle, tumor-to-blood and tumor-to-brain) ratios of [^{18}F](2*S*,4*S*)4-FPGln, **4**, were 6.91, 1.45 and 5.53, respectively. The highest uptake of

[^{18}F](2*S*,4*S*)4-FPGln, **4**, was found in the pancreas. High pancreatic uptake is consistent with the fact that amino acids are precursors for digestive enzymes actively produced in the pancreas.

Low bone (femur) uptake was observed at 30 minutes (0.53% dose/g) and it stayed at that value at 60 min post injection.

Table 1: Tissue distribution of radioactivity (% dose/g) in F344 rats bearing 9L tumors after intravenous injection of [^{18}F](2*S*,4*S*)4-FPGln, **4**. Results are expressed as mean ± SD (n =4).

Organ	30 min	60 min
Blood	0.57 ± 0.02	0.38 ± 0.02
Heart	0.31 ± 0.01	0.26 ± 0.02
Muscle	0.12 ± 0.01	0.11 ± 0.01
Lung	0.52 ± 0.01	0.39 ± 0.02
Kidney	12.4 ± 1.02	8.93 ± 0.42
Pancreas	3.22 ± 0.42	2.24 ± 0.06
Spleen	0.59 ± 0.02	0.42 ± 0.03
Liver	1.72 ± 0.07	1.58 ± 0.08
Skin	0.47 ± 0.15	0.37 ± 0.06
Brain	0.15 ± 0.00	0.16 ± 0.01
Bone	0.53 ± 0.08	0.56 ± 0.17
9L Tumor	0.83 ± 0.04	0.60 ± 0.06
Tumor/Blood	1.45 ± 0.08	1.57 ± 0.17
Tumor/Muscle	6.91 ± 0.66	5.45 ± 0.73

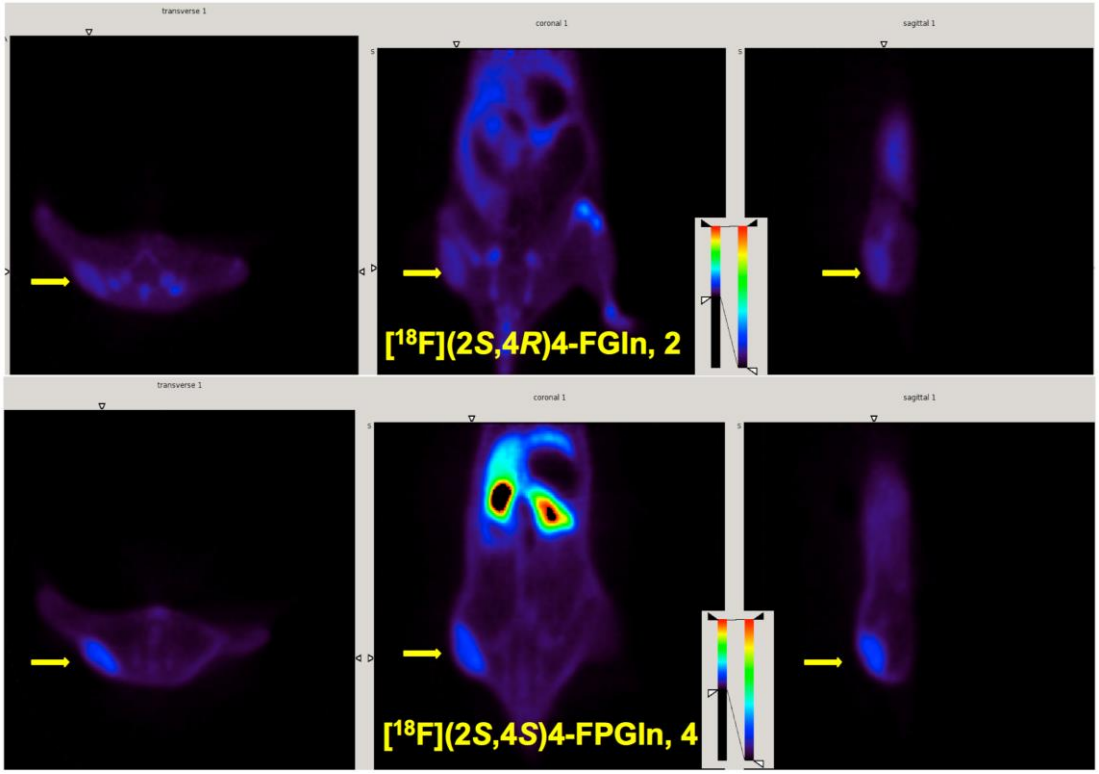

Figure 7. Representative PET images of 9L tumor bearing rats after intravenous injection of [^{18}F](2*S*,4*S*)4-FPGln, **4**, or [^{18}F](2*S*,4*R*)-4FGln, **2**, into a F344 rat bearing a 9L tumor. The images of the transverse, coronal and sagittal views are from a summed 2 h scan. Arrows represent the location of tumors on the hind leg region of the F344 rat.

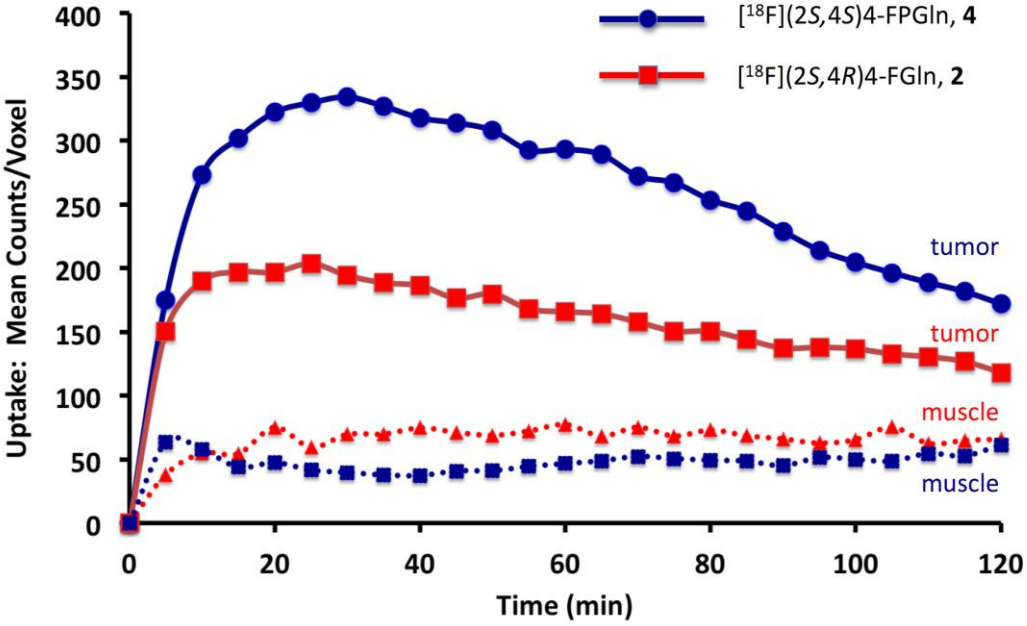

Figure 8. Time activity curves of tumor (target) and muscle (background) uptake in F344 rats bearing 9L tumors: (blue) [^{18}F](2*S*,4*S*)4-FPGln, **4**, and (red) [^{18}F](2*S*,4*R*)4-FGln, **2**.

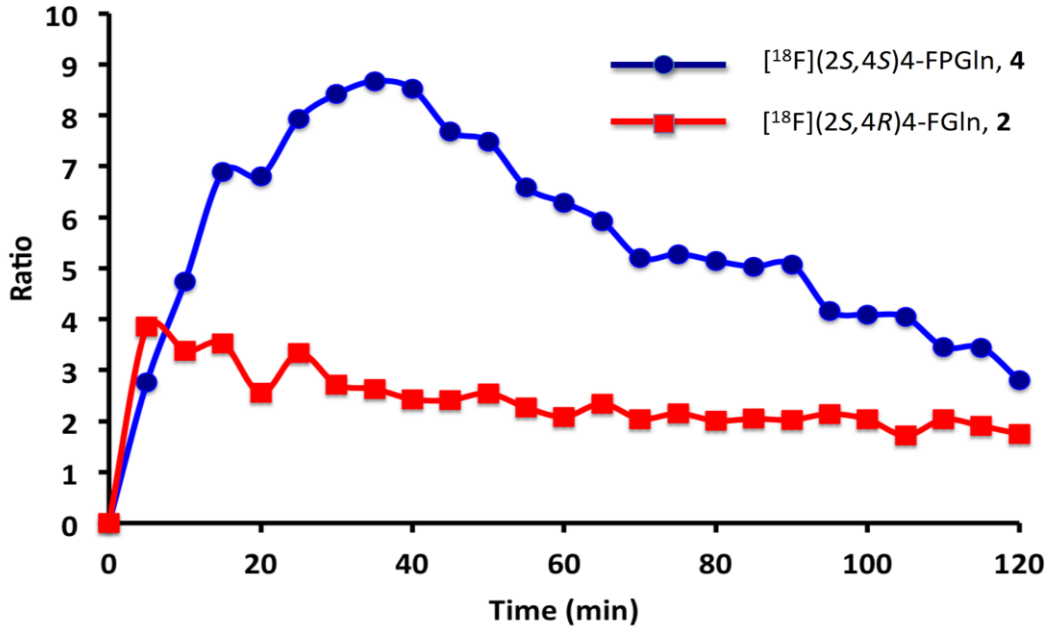

Figure 9. Comparison of ratios of tumor/muscle at different time points (0 min to 120 min) for [^{18}F](2*S*,4*S*)4-FPGln, **4**, and [^{18}F](2*S*,4*R*)4-FGln, **2**.

Preliminary PET imaging studies of [^{18}F](2*S*,4*S*)4-FPGln, **4**, in rats with 9L tumors showed that the probe was clearly taken up by the tumors (n = 3) (Figure 7). To further investigate the tumor uptake, dynamic small animal PET studies using one rat bearing two 9L tumors were carried out

on two different days with either [^{18}F](2*S*,4*S*)4-FPGln, **4**, or [^{18}F](2*S*,4*R*)4-FGln, **2**. The direct comparison study using the same animal can avoid some of the complications related to differences in tumor growth in different animals. [^{18}F](2*S*,4*R*)4-FGln, **2**, was recently reported as a tumor PET imaging agent for glutaminolysis. PET images of [^{18}F](2*S*,4*S*)4-FPGln, **4**, and [^{18}F](2*S*,4*R*)4-FGln, **2** were selected for visualization (Figure 7). As these images demonstrate, the 9L tumors could be visualized with either of the ligands. High kidney, liver and bladder uptake were also observed. Defluorination/bone uptake was more apparent in the images of [^{18}F](2*S*,4*R*)4-FGln, **2**, compared to those of [^{18}F](2*S*,4*S*)4-FPGln, **4**. To assess the *in vivo* kinetics, region-of-interest analysis was performed (using AMIDE software to generate the time-activity curves). The kinetic curves confirmed that all the tracers exhibited higher tumor uptake compared to the muscle (background) regions. [^{18}F](2*S*,4*S*)4-FPGln, **4**, showed a higher tumor-to-muscle ratio than [^{18}F]4-FGln. Both ligands displayed similar kinetics. Both ligands had rapid tumor uptake and reached their maximum uptake within the first 20 min. Tumor uptake for [^{18}F]4-FGln remained rather consistent over 2 h, while [^{18}F](2*S*,4*S*)4-FPGln, **4**, displayed a faster tumor washout rate. Also noteworthy, ([^{18}F](2*S*,4*S*)4-FPGln, **4**, showed less defluorination/bone uptake in comparison to that of [^{18}F]4-FGln. Results of the *in vivo* PET imaging studies using the 9L tumor model suggested that the [^{18}F](2*S*,4*S*)4-FPGln, **4**, localized in the 9L tumor as well, if not better, than [^{18}F](2*S*,4*R*)4-FGln, **2**.

In summary, a new glutamine analog, [^{18}F](2*S*,4*S*)4-FPGln, **4**, has shown tumor specific uptake *in vitro* and *in vivo*. However, the tumor uptake and retention mechanisms may be significantly different from other glutamine probes, such as [^{11}C]Gln, **1** and [^{18}F](2*S*,4*R*)4-FGln, **2**.